Reproduction, 2026, **171**(1), xaaf009
https://doi.org/10.1093/reprod/xaaf009
Research Paper

Society for Reproduction and Fertility

Exploring QRICH2 as a potential male contraceptive target

Amandine Delnatte[1], Messaline Inglese[1], Jérôme Delroisse[2], Denis Nonclercq[3], Annica Frau[3], Ruddy Wattiez[4], Baptiste Leroy[4], Vanessa Arcolia[5], Jean-François Simon[5], Thibault Masai[1], and Elise Hennebert[1,*]

[1]Laboratory of Cell Biology, Research Institute for Biosciences, Research Institute for Health Sciences and Technology, University of Mons, Mons 7000, Belgium
[2]Biology of Marine Organisms and Biomimetics Unit, Research Institute for Biosciences, University of Mons, Mons 7000, Belgium
[3]Laboratory of Histology, Research Institute for Health Sciences and Technology, University of Mons, Mons 7000, Belgium
[4]Laboratory of Proteomics and Microbiology, Research Institute for Biosciences, University of Mons, Mons 7000, Belgium
[5]Clinique de Fertilité Régionale de Mons, CHU HELORA, Mons 7000, Belgium
*Corresponding author: Laboratory of Cell Biology, Research Institute for Biosciences, Research Institute for Health sciences and Technology, University of Mons, Place du Parc 20, Mons 7000, Belgium. Email: elise.hennebert@umons.ac.be
A.D. and M.I. are co-first authors.

In brief

Current male contraceptive options are limited, highlighting the need for novel approaches. This study characterizes the sperm protein QRICH2 in humans, showing its testis-specific expression and key roles in spermatogenesis and sperm structure, suggesting that it may be a promising and safe target for male contraception.

Abstract

Today, male contraceptive options remain limited to condoms and vasectomy, highlighting the urgent need for alternative methods. In this context, discovering and characterizing reproductive-tract-specific proteins that can be targeted by natural or chemical molecules is of particular interest. Recent studies on the sperm protein glutamine-rich protein 2 (QRICH2) show that it could represent a promising candidate. Indeed, it has been genetically confirmed to be essential for male fertility in mice, bulls, and humans, with gene knockout and loss-of-function mutations leading to defective sperm and complete infertility without evident accompanying symptoms. However, information on human QRICH2 remains limited. In this study, we aimed to better characterize human QRICH2 to assess its potential as a target for male contraceptive development. Using mass spectrometry, we assessed which of the QRICH2 isoforms described in databases might be expressed in human sperm. Through in silico analyses, we showed that QRICH2 has no paralogs in humans, and is conserved across mammals, particularly in a region containing two functional domains, suggesting their importance for QRICH2 function. Finally, using immunodetection methods and proteomic dataset analyses, we investigated the tissue specificity of QRICH2 by examining its protein expression across 12 human organs. Our results show that QRICH2 is restricted to the testes, where it localizes to different cellular compartments throughout spermatogenesis, and acts as a cytoskeletal component in mature sperm, both in the head and flagellum. We conclude that QRICH2 represents a promising candidate for further investigation as a potential target for male contraception and we propose different strategies that could be explored for its inhibition.

Keywords QRICH2, humans, male contraception, non-hormonal contraceptive target, testis-specific expression, spermatogenesis

Introduction

Despite four decades of research, male contraceptive methods remain limited (Thirumalai & Amory, 2021). Currently, only condoms and vasectomy offer reliable contraception for men, reflecting a significant gap in contraceptive options compared to those available for women (Kim *et al.*, 2024). Since vasectomy is considered relatively invasive and difficult to reverse, most men rely on condoms for contraception. This disparity in the availability of male contraceptive methods highlights the urgent need for further research and development in this field. Surveys have shown that a significant proportion of men believe contraceptive responsibility should be shared between the sexes and express interest in new male contraceptive options (Nickels & Yan, 2024). In response to this demand, extensive research over the past few decades has focused on developing both hormonal and non-hormonal male contraceptives (Louwagie *et al.*, 2023). However, clinical trials of hormonal contraceptives for men have revealed various side effects (Wang *et al.*, 2016), as well as inconvenient and restrictive administration methods such as injections or the need to take multiple

Received: August 25, 2025; **Revised:** October 24, 2025; **Accepted:** November 4, 2025

pills daily to maintain effectiveness. Moreover, given the recency of these studies, the long-term risks associated with hormonal contraceptive use remain unclear, leaving the acceptable risk–benefit ratio undetermined (Thirumalai & Page, 2020). As a result, non-hormonal approaches are preferred. These consist of either mechanical methods or drug-based strategies. Mechanical methods include barrier methods, thermal methods approaches, and vas-occlusion techniques such as RISUG® (reversible inhibition of sperm under guidance), an intravasal injectable polymer that has demonstrated high efficacy and safety in phase III clinical trials in India (Khilwani *et al.*, 2020; Lohiya *et al.*, 2022). Drug-based methods, on the other hand, aim to target proteins essential for male fertility, ideally with minimal to no side effects (Louwagie *et al.*, 2023). To address these safety concerns, target proteins are selected based on their specificity to the male reproductive system and the absence of paralogs in somatic cells, thereby reducing the risk of undesirable off-target effects (Kent *et al.*, 2020). Furthermore, particular attention is given to proteins whose gene impairment in animal models or patients leads to sterility, ensuring that inhibiting the target protein would achieve effective contraception (Kent *et al.*, 2020). Recent results on the sperm protein glutamine-rich protein 2 (QRICH2) make this protein a potential target as it appears to meet the above-mentioned criteria (Shen *et al.*, 2019).

QRICH2's role was discovered recently in the context of genetic mutations responsible for multiple morphological abnormalities of the flagella (MMAF), a syndrome leading to male infertility (Kherraf *et al.*, 2019; Shen *et al.*, 2019; Hiltpold *et al.*, 2022). In humans and bulls, homozygous mutations in the QRICH2 gene lead to the synthesis of truncated proteins, resulting in severe flagellar deformities, decreased sperm count in the semen, and immotile sperm (Kherraf *et al.*, 2019; Shen *et al.*, 2019; Hiltpold *et al.*, 2022). In addition, QRICH2 knock-out (KO) male mice are infertile and display a MMAF phenotype without evident accompanying symptoms (Shen *et al.*, 2019). Further analysis of these KO mice revealed that the reduced sperm count is not due to impaired meiosis, but rather to elevated levels of reactive oxygen species, which induce DNA damage in spermatids and lead to their subsequent autophagy and apoptosis (Zhang *et al.*, 2024b). In view of these findings, QRICH2 appears to play a crucial role in sperm flagellum biogenesis and in protecting spermatids from excessive reactive oxygen species-induced damage (Shen *et al.*, 2019; Zhang *et al.*, 2024b). The former function is in part explained by QRICH2's ability to regulate proteins involved in flagellum development: it activates the transcription of ODF2 and CABYR and inhibits the ubiquitin-proteasome dependent degradation of ROPN1, AKAP3, TSSK4, and MARCH10 (Shen *et al.*, 2019).

The objective of this study is to further characterize human QRICH2 to evaluate if it could be used as a male contraceptive target. Indeed, to date, most of the available data on QRICH2 have been obtained in mice (Shen *et al.*, 2019; Zhang *et al.*, 2024a; 2024b), while information on the human protein remains limited. In this study, we examined QRICH2's tissue specificity at the protein level and analyzed its localization during spermatogenesis as well as in ejaculated sperm. Using sperm protein extraction combined with mass spectrometry (MS), we determined QRICH2's primary structure, enabling discrimination between the several isoforms described in databases. Finally, through in silico analyses, we investigated the presence of QRICH2 paralogs in somatic cells and the evolutionary conservation of QRICH2 proteins across mammals.

Materials and methods

Samples and ethics

Human semen samples were obtained from the fertility clinic of HELORA Hospital (Mons, Belgium) from patients undergoing routine semen analysis or from voluntary donors. All experiments conducted in this study were approved by the Ethics Committee of HELORA Hospital in Mons and by the Ethics Committee of Erasme Hospital in Brussels (EudraCT/CCB:/B4062024000219). The samples were obtained with the informed written consent of all subjects. Semen samples were collected by masturbation after an abstinence period of 3–5 days and routine semen analysis was performed according to the World Health Organization 2021 guidelines (WHO, 2021). Only normozoospermic samples (volume ≥ 1.4 mL, sperm concentration ≥ 16×10^6/mL, and total motility ≥ 42%) were investigated. Sperm purification from the semen samples was carried out by centrifugation at 300 × g for 20 min at 37 °C on a discontinuous PureSperm 40/80 density gradient (Nidacon, Mo¨lndal, Sweden) as described in Nicholson *et al.* (2000) and the World Health Organization guidelines (WHO, 2021). Purified sperm recovered from the bottom of the 80% PureSperm fraction were then washed with Dulbecco's phosphate-buffered saline (DPBS; Sigma-Aldrich, St Louis, MO, U.S.A.) supplemented with 100 µg/mL ampicillin (Thermo Fisher Scientific, Geel, Belgium).

Sections from human testis, epididymis, cerebral cortex, heart, colon, pancreas, lung, kidney, thyroid, and prostate fixed in formalin and embedded in paraffin were obtained from Erasme Hospital biobank [BE_BERA1; Biobanque Hôpital Erasme-Université Libre de Bruxelles (BERA); BBMRI-ERIC]. The sections were taken from tissues sampled at a distance from a malignant region and presenting a normal histology (i.e., complete spermatogenesis in the case of testes).

Sperm protein extraction and western blot analysis

Proteins were extracted from freshly purified sperm using different buffers: (1) Laemmli sodium dodecyl sulfate (SDS) sample buffer [50 mM Tris, 10% (v/v) glycerol, 2% (w/v) SDS, 50 mM dithiothreitol (DTT), bromophenol blue, pH 6.8], (2) RIPA without SDS [50 mM Tris, 150 mM sodium chloride (NaCl), 1% Triton-X-100, 0.25% sodium deoxycholate, pH 7.5], (3) RIPA with SDS (50 mM Tris, 150 mM NaCl, 1% Triton-X-100, 0.25% sodium deoxycholate, 0.1% SDS, pH 7.5), (4) DPBS with 1% Triton-X-100, and (5) urea buffer (50 mM K_2HPO_4, 8 M urea, 50 mM DTT, pH 8.5), all supplemented with protease inhibitors (Complete ULTRA Tablets; Roche, Mannheim, Germany). For the first buffer, the sample was incubated in the buffer for 5 min at room temperature and then at 95 °C for 5 min. For the other buffers, the samples were vortexed three times for 10 s each and then submitted to mechanical lysis using an ultrasound probe (IKA U50 sonicator). Three cycles of sonication of 5 s at 20% amplitude were performed at 4 °C. The samples were centrifuged briefly and incubated for 30 min on ice or at room temperature in the case of the urea buffer. They were then centrifuged at 17,000 x g for 15 min at 4 °C or room temperature. The supernatants were then mixed with Laemmli SDS sample buffer (containing 100 mM DTT) and heated for 5 min at 95 °C. All the extracts were centrifuged and loaded on 5% or 8% sodium

dodecyl sulfate–polyacrylamide gel electrophoresis (SDS-PAGE) gels. Electrophoresis was carried out with TGS buffer [25 mM Tris, 192 mM glycine, 0.1% (w/v) SDS].

For western blot analysis, proteins separated by electrophoresis were transferred onto PVDF membranes (GE Healthcare) using 25 mM Tris, 192 mM glycine, 0.05% (w/v) SDS, 20% (v/v) methanol as transfer buffer. The membranes were washed with phosphate-buffered saline containing 0.05% (v/v) Tween 20 (PBS-Tw) and then blocked for 1 h in PBS-Tw containing 5% (w/v) bovine serum albumin (PBS-Tw-BSA) (Carl Roth GmbH, Karlsruhe, Germany). After that, they were incubated overnight at 4 °C under gentle agitation with a rabbit polyclonal anti-QRICH2 antibody (Atlas antibodies AB, Bromma, Sweden; Cat# HPA052219) diluted 1:1000 in PBS-Tw-BSA (3%). After five washes of 5 min each in PBS-Tw, the membranes were incubated for 1 hr at room temperature under gentle agitation with horseradish peroxidase-conjugated goat anti-rabbit immunoglobulins (Proteintech, Manchester, UK; Cat# SA00001-2) diluted 1:5000 in PBS-Tw-BSA (3%). Finally, the membranes were washed again and immunoreactive bands were visualized using the ECL western blotting substrate (Thermo Fisher Scientific, Waltham, MA, U.S.A.) or the SuperSignal™ West Femto maximum sensitivity substrate (Thermo Fisher Scientific, Waltham, MA, U.S.A.) and the Fusion FX imaging system (Vilber, Marne-la-Vallée, France).

MS analyses

Proteins extracted from freshly purified sperm using Laemmli SDS sample buffer were resolved on a 4–20% (w/v) MiniPROTEAN TGX precast polyacrylamide gel (Bio-Rad Laboratories; Hercules, CA, U.S.A.). One part of the gel was used for western blot analysis as described above to assess the presence of QRICH2. The other part of the gel was stained using Coomassie brilliant blue R-250 and the gel band corresponding to QRICH2 (as determined by western blot) was excised. The gel band was washed twice in 25 mM ammonium bicarbonate (ABC buffer) and then twice in ABC buffer containing 50% (v/v) acetonitrile (acetonitrile buffer), each time for 15 min under agitation. It was then incubated in 50 mM DTT in ABC buffer at 56 °C for 45 min and subsequently in 50 mM iodoacetamide in ABC buffer in the dark for 30 min. Again, the gel band was washed twice in ABC buffer and then twice in acetonitrile buffer. It was then incubated in 15 µL of a digestion solution made up of 10 ng/µL of porcine sequencing grade modified trypsin (Promega, Madison, WI, U.S.A.) in ABC buffer. This incubation was first performed for 30 min at 4 °C and then overnight at 37 °C. After digestion, to maximize peptide recovery, the supernatant was collected, and the gel band was subsequently incubated for 15 min in ABC buffer, followed by 15 min in acetonitrile buffer containing 5% (v/v) formic acid. All three resulting supernatants were pooled. The combined supernatant, containing the tryptic peptides, was then air-dried using a DNA120 OP DNA SpeedVac™ Concentrator (Thermo Fisher Scientific, Geel, Belgium) and stored at −20°C. Before analysis, the peptides were resuspended in 10 µl of a solution containing 2% (v/v) acetonitrile and 0.1% (v/v) formic acid. The sample was then centrifuged at 17,000 x g for 20 min at 4 °C and tryptic peptides were analyzed by reverse-phase HPLC-ESI-MS/MS on a UHPLC-HRMS/MS instrument (AB SCIEX LC420 and TripleTOF 6600) using the DDA mode of acquisition. Tryptic peptides were separated on a C18 column (YMC-Triat 0.3 mm × 150 mm column) with a linear acetonitrile gradient (5% to 35% of acetonitrile, 5 µL.min^{-1}, 20 min) in water containing 0.1% formic acid. MS survey scans (m/z 400–1250, 100 ms accumulation time, mass resolution of ±25,000) were followed by 50 MS/MS acquisition. Collision-induced dissociation was carried on using rolling collision energy, and fragment ions were accumulated for 50 ms in high-sensitivity mode (mass resolution of ±10,000). MS/MS data were processed with ProteinPilot software (version 5.0.1.0,4895, AB SCIEX) and analyzed against the Uniprot *Homo sapiens* database (release 2022_05) with the relevant parameters, including carbamidomethyl cysteine, oxidized methionine, all biological modifications, amino acid (aa) substitutions, and missed cleavage site. Only proteins identified with <1% false discovery rate were considered.

Construction of expression vectors encoding QRICH2 isoforms

Expression vectors were obtained by Gateway® Recombination Cloning Technology (Thermo Fisher Scientific, Geel, Belgium). First, pENTR vectors encoding three human QRICH2 isoforms, Q9H0J4, A0A1B0GW36, and A0A7P0T7G7 (UniProt) were obtained as follows. The pENTR containing the sequence coding for the Q9H0J4 isoform was purchased from Horizon Discovery Ltd (Cambridge, U.K.), which holds a copy of the Human ORFeome Collection, a collection of plasmids containing most of the open reading frames (ORFs) of the human genome (Lamesch *et al.*, 2007; ORFeome Collaboration, 2016). The pENTR plasmid encoding isoform A0A1B0GW36 was obtained by modification of the pENTR encoding the Q9H0J4 isoform. The sequence coding isoform A0A1B0GW36 contains an additional 496 nucleotides at the 5′ end compared to the sequence coding for isoform Q9H0J4. To modify the pENTR coding for isoform Q9H0J4, two restriction sites for the Bsp120I enzyme were identified in this pENTR: one upstream of the Q9H0J4 ORF, within the plasmid backbone sequence, and the other in the 5′ region of the Q9H0J4 ORF, which is shared with the ORF of A0A1B0GW36. A synthetic gene corresponding to the nucleotide sequence between the two restriction sites was purchased from Integrated DNA Technologies (Leuven, Belgium) as a gBlock. This synthetic gene was then inserted into the pENTR coding for Q9H0J4 by restriction/ligation cloning. The pENTR plasmid encoding isoform A0A7P0T7G7 was obtained by modification of the pENTR encoding the A0A1B0GW36 isoform. The sequence coding for isoform A0A7P0T7G7 contains an additional 174 nucleotides at the 3′ end compared to the sequence coding for isoform A0A1B0GW36. To modify the pENTR containing the ORF coding for isoform A0A1B0GW36, two restriction sites were identified. The first, recognized by the Eco147I enzyme, is located at the 3′ end of the ORF coding for the protein, and the second, recognized by the Eco32I enzyme, is located downstream of the ORF, within the plasmid backbone. A synthetic gene corresponding to the nucleotide sequence between the two restriction sites, including the sequence comprising the missing 174 nucleotides, was purchased from Integrated DNA Technologies (Leuven, Belgium) as a gBlock. This synthetic gene was then integrated into the pENTR coding for isoform A0A7P0T7G7 by restriction/ligation cloning. For the construction of the expression vectors, LR reactions between the pENTR vectors and the pDEST vector pCMV-Cter_3flag-RFAgw were performed using LR Clonase® enzyme (Thermo Fisher Scientific,

Geel, Belgium). The three expression plasmids were verified using Sanger sequencing (Eurofins Genomics, Konstanz, Germany). pCMV-Cter_3flag-RFAgw was obtained from MGC, IGMM Montpellier. It was generated by introducing the RFA Gateway cassette into p3x-FLAG-CMV-14 (Merck KGaA, Darmstadt, Germany; Cat# E7908).

Production of QRICH2 isoforms in human embryonic kidney 293T cells

Human embryonic kidney (HEK) 293T cells (ATCC #CRL-11268) were maintained at 37 °C and 5% CO_2 in Dulbecco's modified eagle's medium high glucose (DMEM, PAN-Biotech GmbH, Aidenbach, Germany) supplemented with 10% decomplemented fetal bovine serum (FBS, Biochrom GmbH, Berlin, Germany) and 1% of antibiotics (10,000 units/mL penicillin and 10,000 µg/mL streptomycin, Gibco, Life Technologies Corporation, Grand Island, NY, U.S.A.). At 24 hr before transfection, 1 x 10^5 cells were plated onto 24-well plates and incubated at 37 °C in 5% CO_2. Cells grown to 60–80% confluence were transfected with the expression vectors using jetPRIME transfection reagent (PolyPlus, Illkirch, France). Cells were lysed 48 hr post-transfection in a lysis buffer (50 mM Tris, 250 mM NaCl, 2 mM EDTA, 1% Triton-X-100, pH 7.4) supplemented with protease inhibitors. The extracts were then analyzed by western blot, as described in the *Sperm protein extraction and western blot analysis* section, to detect QRICH2.

In silico analyses

In silico analyses were performed using QRICH2's longest isoform, i.e., A0A7P0T7G7. The presence of conserved domains was predicted by the NCBI Conserved Domain Database v3.21 (CDD) (Wang *et al.*, 2023). To identify QRICH2 paralogs in humans, a BLASTp (Altschul *et al.*, 1990) search was performed using the human QRICH2 sequence in the NCBI non-redundant database (release 266), restricting the search to *Homo sapiens*. To assess the conservation of QRICH2 in mammals, a subset of mammalian QRICH2 protein sequences, selected from 16 different species across 14 mammalian orders, was selected. A pairwise alignment was performed between the protein sequence of each species and the protein sequence of *H. sapiens* using the Geneious global alignment algorithm (based on Needleman-Wunsch; cost matrix: Blosum 62), as implemented in Geneious Prime 2025.1.3. For each 200-aa region of human QRICH2, distance matrices representing the percentage of identity between species were retrieved. Selected species and respective orders were: *Macaca mulatta* (Primates), *Pan troglodytes* (Primates), *Rattus norvegicus* (Rodents), *Mus musculus* (Rodents), *Bos taurus* (Artiodactyls), *Canis lupus familiaris* (Carnivores), *Oryctolagus cuniculus* (Lagomorphs), *Equus caballus* (Perissodactyls), *Orcinus orca* (Cetaceans), *Elephas maximus indicus* (Proboscideans), *Phyllostomus discolor* (Chiropterans), *Dromiciops gliroides* (Microbiotheres), *Sarcophilus harrisii* (Dasyuromorphs), *Sorex fumeus* (Soricomorphs), *Manis javanica* (Pholidotes), and *Choloepus didactylus* (Pilosa).

Then, to analyse the global conservation of QRICH2 across mammals, vertebrates, and eukaryotes, homolog protein sequences of QRICH2 were retrieved from the OrthoDB database (v12.1, July 10, 2025) (Kriventseva *et al.*, 2019), using "QRICH2" as the query. Three taxonomic datasets were extracted: sequences restricted to mammals (272 sequences), vertebrates (1645 sequences), and eukaryotes (4629 sequences). The human QRICH2 sequence (isoform A0A7P0T7G7) was included as reference in each alignment. Each dataset was aligned separately using MAFFT (v7.515) with the default automated methods (FFT-NS-2 strategy) (Katoh *et al.*, 2017). Non-trimmed alignments were analysed for comparison. Only columns aligned to the human sequence A0A7P0T7G7 (i.e., non-gap in the human QRICH2 sequence) were considered to ensure accurate positional correspondence. Normalized Shannon entropy was calculated for each alignment column to estimate conservation using the formula: $H = -\sum_i p_i \log_2(p_i)$, where pi is the frequency of aa i at that position. Conservation scores were derived as $1-H/H\text{max}1$, where Hmax is the maximum entropy over 20 amino acids. The analysis was restricted to the 20 standard amino acids. Sequence coverage (i.e., the proportion of non-gap characters per column) was computed in parallel. Conservation and coverage scores were mapped onto the human reference sequence positions. The three annotated protein domains of human QRICH2 A0A7P0T7G7, based on CDD predictions, were highlighted in all analyses. We developed an R script (available upon request) that computes two parameters per alignment column: (1) conservation score, calculated as 1 minus the normalized Shannon entropy of aa frequencies at each position (Capra & Singh, 2007), and (2) alignment coverage, defined as the proportion of sequences without a gap at that position. For visualisation purposes, smoothed conservation and coverage curves were computed using a centered moving average with a 50-aa window to improve readability and reduce noise. The human QRICH2 reference sequence was used to anchor alignment positions. Plots were generated with ggplot2 in R.

Detection of QRICH2 in published human organ proteomes

The presence of QRICH2 was investigated in published proteomes from ten human organs (testis, brain, heart, colon, liver, pancreas, skin, lung, prostate, and thyroid). These organs were selected based on (1) their representation of major physiological systems and (2) the availability of multiple high-quality proteomic datasets. To find relevant articles on organ proteomes, the following search terms "human + [organ name] + proteome" were used in Google Scholar and PubMed. The ProteomeXchange repository (Deutsch *et al.*, 2023) was also consulted by searching for all available proteomes for each organ in *H. sapiens*. For each organ, at least four different proteomes were selected based on the following criteria: (1) inclusion of non-cancerous tissue, not limited to cancerous samples; (2) for complex organs (e.g., the brain), inclusion of proteomes from different regions; and (3) preference for studies using most recent, high-sensitivity methodologies in combination with state-of-the-art MS technologies.

Analysis of QRICH2 localization on human organ sections and sperm

The presence of QRICH2 in ten human organs (testis, epididymis, cerebral cortex, heart, colon, pancreas, lung, kidney, thyroid, and prostate), selected based on tissue availability in the Biobank,

was investigated by immunofluorescence (IF) and immunohistochemistry (IHC). Sections from the different organs (5 µm in thickness) were dewaxed and rehydrated. For each tissue, one section was stained using Masson's trichrome to evaluate tissue histology, and the others were subjected to IF and IHC methods according to the following protocol. First, heat-induced epitope retrieval was performed with sodium citrate buffer (21.8 mM citric acid, pH = 6.2). Sections were washed with PBS before blocking in PBS-BSA (5%). They were then incubated overnight at 4 °C with rabbit polyclonal anti-QRICH2 (Atlas antibodies AB, Bromma, Sweden; Cat# HPA052219) diluted 1:100 in PBS-Tw-BSA (3%). Controls were performed by incubating sections in PBS-Tw-BSA (3%) without primary antibody. Following several washes with PBS-Tw, the sections were incubated for 1 hr at room temperature with Alexa fluor 568-coupled goat anti-rabbit immunoglobulins (Invitrogen, Eugene, OR, U.SA.; Cat# A-11011) diluted 1:100 in PBS-Tw-BSA (3%). For testis sections, acrosome labelling was performed for 30 min at room temperature with a 5 μg/mL solution of fluorescein isothiocyanate (FITC) conjugated *Pisum sativum* agglutinin (PSA-FITC; Sigma-Aldrich, Burlington, MA, U.S.A.; Cat# L0770) in PBS. Finally, the sections were counterstained for 15 min with 10 µg/mL of Hoechst 33342 (Sigma-Aldrich, St Louis, MO, U.S.A.) and mounted with Vectashield Plus Antifade Mounting Medium (Vector Laboratories, Burlingame, CA, U.S.A.; Cat# H-1900). To detect Sertoli cells unambiguously, some testis sections were exposed to double immuno-labelling for QRICH2 and vimentin using the same protocol but with serial incubations with (1) mouse monoclonal anti-vimentin (Proteintech, Manchester, U.K.; Cat# 60330-1-Ig) diluted 1:500 in PBS-BSA (3%) for 2 hr at room temperature, (2) rabbit polyclonal anti-QRICH2 overnight at 4 °C, (3) Alexa fluor 568-coupled goat anti-rabbit immunoglobulins for 1 hr at room temperature, and (4) CoraLite488 conjugated Affinipure Goat Anti-Mouse (Proteintech; Cat# SA00013-1) diluted 1:100 in PBS-BSA (3%) for 1 hr at room temperature. Z-Stack images of 0.1 µm increment were collected using a confocal microscope (Nikon TI2-E-A1RHD25). For IHC, the secondary antibody was an ImmPRESS anti-rabbit immunoglobulin G horseradish peroxidase (MP-7401; Vector Laboratories, Burlingame, CA, U.S.A.), used undiluted for 30 min at room temperature. After washing, sections were incubated in a 0.05% (w/v) hydrogen peroxide (Sigma-Aldrich Chemie GmbH, Steinheim, Germany; Cat# 95314) containing 0.49 mg/mL diaminobenzidine (Sigma-Aldrich Chemie GmbH, Steinheim, Germany; Cat# D5637), until immunostaining development. Sections were counterstained with hemalun and luxol fast blue, dehydrated and mounted with a permanent mounting medium (Richard-Allan Scientific, Kalamazoo, MI, U.S.A.; Cat# 4112), and observed using a Zeiss Axioscope A1 microscope.

Aliquots of purified sperm were fixed in an equal volume of 4% (w/v) paraformaldehyde (Sigma-Aldrich, Burlington, MA, U.S.A.) in PBS for 20 min at room temperature. The samples were then centrifuged at 2000 x g for 5 min at 4 °C. They were washed twice with PBS supplemented with 50 mM glycine, to quench the remaining paraformaldehyde, and once with PBS. Droplets of 0.1 to 0.2×10^6 fixed sperm were air-dried on 12 mm diameter glass coverslips. After a quick wash with PBS-Tw, sperm were permeabilized in PBS-Tw containing 0.3% (v/v) Triton X-100 (Carl Roth GmbH, Karlsruhe, Germany) for 20 min. They were then subjected to IF as described above. In this case, controls were performed by replacing the anti-QRICH2 antibody with rabbit IgG (Sigma-Aldrich, St Louis, MO, U.S.A.; Cat# I5006) diluted at 20 µg/mL in PBS-Tw-BSA (3%).

Results

Characterization of native QRICH2 from human sperm

We extracted proteins from human sperm using different buffers and analyzed for the presence of QRICH2 by western blot (Figure 1, and Supplementary Figure S1, see online supplementary material). Notably, only strong denaturing buffers, containing high concentrations of SDS or urea (lanes 1 and 5 in Figure 1, respectively) allowed the extraction of QRICH2, suggesting that the protein is tightly bound within the sperm structure.

As human QRICH2 exists as several isoforms in the Ensembl and UniProt databases, we analyzed native QRICH2 from human sperm by MS to assess which isoform is actually expressed. For this purpose, the gel band corresponding to QRICH2 (as determined by western blot) was excised and submitted to in-gel trypsinolysis. QRICH2 was identified with 35 peptides at >95% confidence (Figure 2, and Supplementary Figure S2 and supplementary Table S1, see online supplementary material). Among these, 31 peptides were common to the three longest isoforms described in databases: Q9H0J4 (1663 aa), A0A1B0GW36 (1829 aa), and A0A7P0T7G7 (1887 aa). Additionally, four peptides matched a sequence absent in Q9H0J4 but present in the N-terminal region of A0A1B0GW36 and A0A7P0T7G7. The first peptide identified in the sequence, PPATTVSLR, lacks the initial methionine residue at its N-terminus (Supplementary Figures S2 and S3 and Supplementary Table S1, see online supplementary material), indicating that it corresponds to the N-terminal end of the protein. Indeed, in eukaryotes, the N-terminal methionine is often co-translationally cleaved by the enzyme methionine aminopeptidase when followed by small residues, including proline, as is the case here (Wingfield, 2017). The A0A1B0GW36 and A0A7P0T7G7 isoforms differ only by the presence of 58 additional aa at the C-terminal end of A0A7P0T7G7, but our MS data did not allow discrimination between them. As western blot analysis of sperm extracts revealed a single distinct high-molecular-weight band (Figure 1) with the polyclonal anti-QRICH2 antibody, which is directed against an immunogen sequence common to all isoforms, these results suggest that only one of these two isoforms is present in sperm.

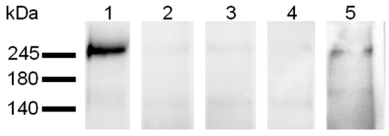

Figure 1 Extraction of QRICH2 from human sperm using different buffers. Proteins were extracted from purified human sperm using: lane 1. Laemmli (50 mM Tris, 10% glycerol, 2% SDS, 50 mM DTT), lane 2. RIPA without SDS (50 mM Tris, 150 mM NaCl, 1% Triton-X-100, 0.25% deoxycholate), lane 3 RIPA with SDS (50 mM Tris, 150 mM NaCl, 1% Triton-X-100, 0.25% deoxycholate, 0.1% SDS), lane 4 DPBS with 1% Triton-X-100, and lane 5 urea buffer (50 mM K_2HPO_4, 8M urea, 50 mM DTT). The protein extracts were resolved by SDS-PAGE (8% acrylamide) and analyzed by western blot using anti-QRICH2 antibodies.

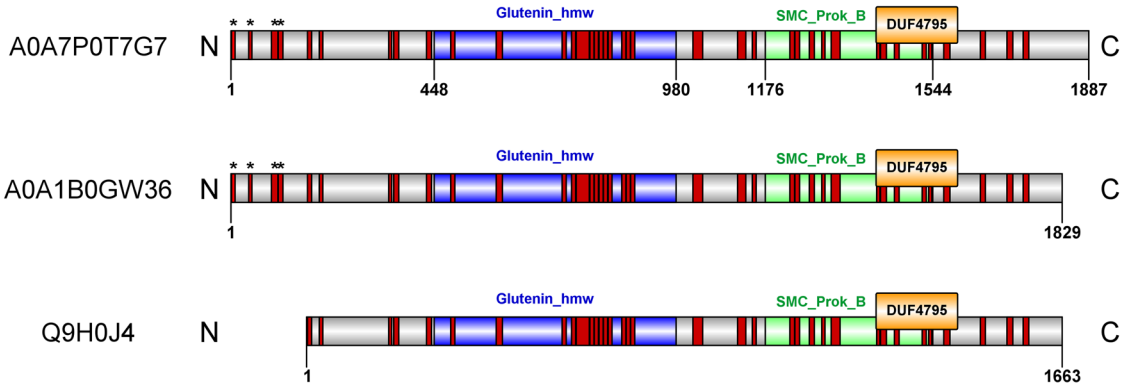

Figure 2 Identification of QRICH2 isoform expressed in human sperm. Human QRICH2 exists as several isoforms in the UniProt database, with the isoform comprising 1663 amino acids (aa) (Q9H0J4) being recognized as the canonical isoform [see also Kherraf *et al.* (2019); Shen *et al.* (2019)]. To discriminate between these isoforms, native QRICH2 from human sperm was analyzed by mass spectrometry following in-gel trypsinolysis. Resulting peptides identified with >95% confidence are indicated in red. Four of them (*) matched the N-terminal part of two isoforms longer than Q9H0J4: A0A1B0GW36 (1829 aa) and A0A7P0T7G7 (1887 aa). The three conserved regions predicted by the Conserved Domain Database are shown: a region with similarity to the superfamily of high molecular weight glutenin subunit (Glutenin hmw; positions 448–980), a region with similarity to the superfamily of chromosome segregation protein SMC (SMC_prok_B; positions 1176–1544), and a domain of unknown function (DUF4795; positions 1419–1598). The SMC_prok-B domain also presents similarity with the YhaN superfamily, of unknown function. Image created using Illustrator for Biological Sequences (IBS) 1.0.3 (Liu *et al.*, 2015).

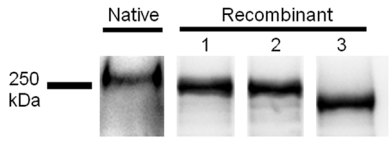

Figure 3 Comparison of native QRICH2 and recombinant isoforms in SDS-PAGE. Proteins were extracted from purified human sperm and from HEK293T cells transfected with expression vectors encoding QRICH2 isoforms A0A7P0T7G7 (lane 1), A0A1B0GW36 (lane 2), and Q9H0J4 (lane 3), each fused to a C-terminal 3XFlag tag. Samples were resolved by SDS-PAGE (5% acrylamide) and analyzed in western blot using anti-QRICH2 antibodies. All extracts were run on the same gel; however, the membrane section with the sperm extract was exposed for a longer time to ensure proper visualization of the QRICH2 band.

Next, we expressed the three isoforms fused to a C-terminal 3xFlag tag in HEK293T cells and compared their apparent molecular weight (MW) to that of native QRICH2 using western blot analysis (Figure 3, and Supplementary Figure S4, see online Supplementary material). The apparent MW of native QRICH2 (256 kDa) was higher than that of the three recombinant isoforms. Interestingly, each protein displayed an apparent MW greater than its calculated one (including the 3xFlag tag): 229 vs 186 kDa for Q9H0J4, 245 vs 204 kDa for A0A1B0GW36, and 248 vs 210 kDa for A0A7P0T7G7. These results suggest that both native and recombinant proteins undergo post-translational modifications (PTMs).

For subsequent in silico analyses, we used the longest isoform, A0A7P0T7G7.

QRICH2 is highly conserved among mammals

QRICH2 contains three functional regions predicted by CDD: a region with similarity to the superfamily of high MW glutenin subunit (Glutenin hmw), a region with similarity to the superfamily of chromosome segregation protein SMC (SMC_prok_B), and a domain of unknown function (DUF4795) (Figure 2).

Pairwise alignment analysis revealed that QRICH2 is highly conserved among mammals (Figure 4A, and Supplementary Table S2, see online Supplementary material). For instance, it shares 95.5% global identity and 97.6% global similarity with QRICH2 from *P. troglodytes* and 46% identity and 64.1% similarity with *M. musculus* (Supplementary Table S2). The three functional domains of human QRICH2 were also detected in most mammalian species (Figure 4B). Interestingly, the region between aa 1400 and 1600 in the human protein is the most conserved, with identity percentages ranging from 73.9% (in killer whales) to 98.5% (in rhesus macaques) (Figure 4). This region includes the C-terminal part of the SMC region and the DUF4795 domain, suggesting a potential functional importance for these domains.

Then, to explore its evolutionary conservation more broadly, we examined QRICH2 across three taxonomic groups: eukaryotes, vertebrates, and mammals. To visualize conservation patterns along the human QRICH2 sequence, we computed normalized Shannon entropy scores per alignment position and plotted smoothed conservation and coverage curves for the non-trimmed alignments (Supplementary Figure S5, see online Supplementary material). Across all datasets, the N-terminal half of the protein—encompassing the glutenin domain—is highly variable, with both low conservation scores and high gap content, indicating poor alignability and extensive sequence divergence. In contrast, the C-terminal region, especially the DUF4795 domain, exhibited markedly higher conservation, particularly among mammals. In this group, the entire DUF4795 region aligns well across species and shows conservation scores near 1.0, suggesting strong evolutionary constraint. In vertebrates, conservation in this region was lower and was accompanied by higher gap frequencies, suggesting weaker alignment confidence and possible structural divergence. The signal was even less pronounced in the eukaryote dataset, where alignment quality appeared limited outside a few short motifs, suggesting lineage-specific divergence. Overall, these analyses show that QRICH2

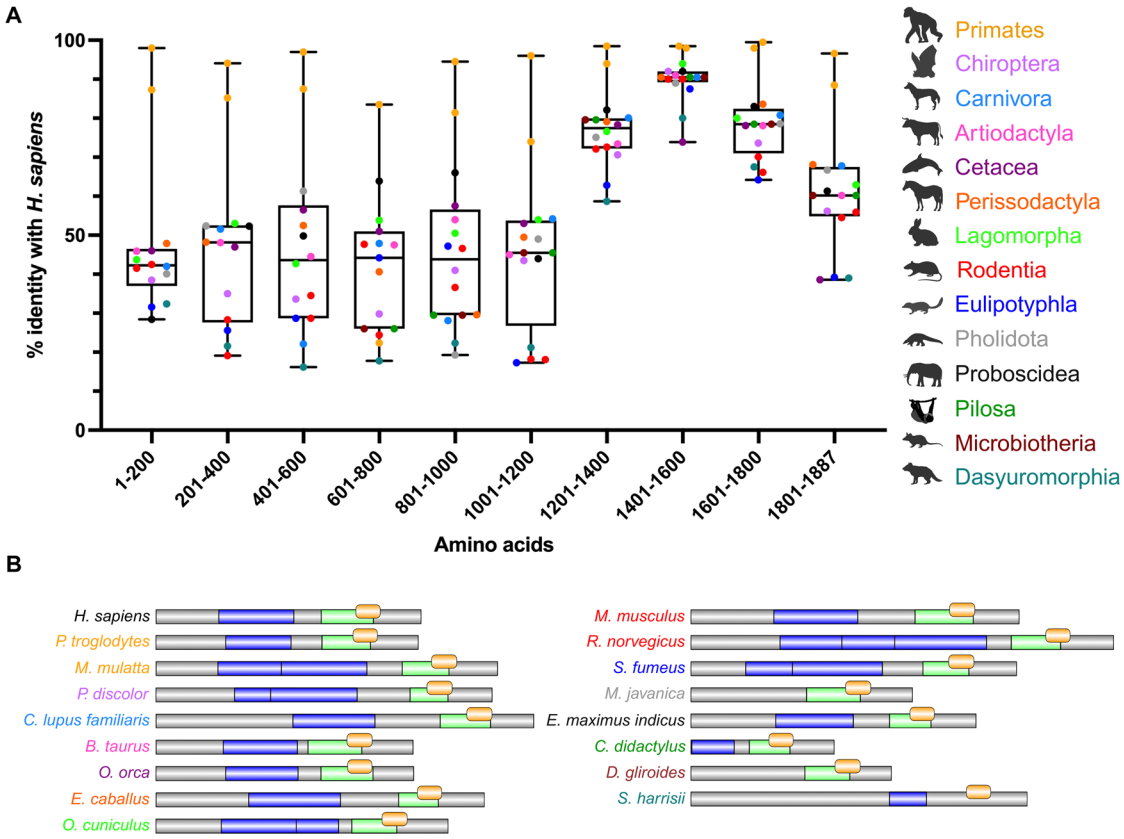

Figure 4 Conservation of QRICH2 across 16 mammalian species. (A) Box plots representing the percentage identity of each of the five 200-amino acid segments of the human QRICH2 protein compared to orthologous QRICH2 sequences from 16 mammalian species, covering 14 distinct orders. Each dot represents one species, color-coded by taxonomic order (legend at right). The line within each box indicates the median; whiskers represent the full data range (minimum to maximum). (B) Schematic representations of QRICH2 from the different species, showing the Glutenin hmw (blue), SMC_prok_B (green), and DUF4795 (yellow) domains.

Table 1 BLASTp hits for QRICH2 in the NCBI non-redundant *Homo sapiens* database.

Description	Accession number	Bit score	Query cover	E value	% Identity	QRICH2 alignment region
Glutamine-rich protein 2 isoform 2 (QRICH2)	NP_001375382.1	3773	100%	0	100	1–1887
Spermidine/spermine N1-acetyl transferase like 1 (SATL1)	KAI2600144.1	424	27%	8.00E−46	34	470–972
Uncharacterized protein C16orf96	NP_001138483.1	109	9%	1.00E−22	34	1420–1599
Piccolo/aczonin (partial) (ACZ)	CAB60727.1	52	10%	6.00E−05	31	660–848

conservation is highly clade-dependent and that the C-terminal region (encompassing DUF4795) stands out as the most conserved segment, particularly in mammals.

QRICH2 has no close paralogs in humans

To investigate the presence of QRICH2 paralogs in humans, we performed a BLASTp search against the NCBI non-redundant database, restricting the search to *H. sapiens*. Apart from QRICH2, only three hits were retrieved: spermidine/spermine N1-acetyl transferase like 1 (SATL1), uncharacterized protein C16orf96, and piccolo/aczonin (ACZ). However, these proteins aligned with only a small region of QRICH2, with low identity (Table 1). These results indicate that QRICH2 lacks sequence homology with other human proteins.

QRICH2 is specific to testes

Although QRICH2 mRNA was exclusively detected in the testes in mice [(Shen *et al.*, 2019), NCBI Gene database, Mammalian Reproductive Genetics (MRG)], in humans, some databases, such as MRG, Human Protein Atlas (HPA), and BGee, report low QRICH2 mRNA levels in other tissues. Here, we aimed to assess the tissue specificity of QRICH2 at the protein level. Indeed, protein levels often correlate poorly with transcript levels (Bauernfeind & Babbitt, 2017; Jiang *et al.*, 2020).

First, we investigated the presence of QRICH2 in ten different human organs using IF and immunohistochemistry (IHC). While a specific immunolabeling was observed in testis sections (Figure 5), no signal was detected in sections from the epididymis, cerebral cortex, heart, colon, pancreas, lung kidney, thyroid, or prostate (see online Supplementary Figures S6–S14, respectively).

To strengthen these findings, we analyzed published proteomes from different organs, as MS provides detection capabilities that complement those of IF and IHC. This analysis focused on organs representative of major physiological systems, including the brain, heart, colon, liver, pancreas, skin, lung, prostate, and thyroid. Except for the skin, where only four datasets met the inclusion criteria defined in the Materials and methods section, five proteomes were analyzed per organ (Supplementary Table S3, see online Supplementary material). Among all the proteomes analyzed, QRICH2 was detected exclusively in the testis. However, it was present in only two of the five testis proteomes, with 11 peptides identified in the dataset by Sun *et al.* (2019) and 7 peptides in that of Zheng *et al.* (2021). The detection of QRICH2 in only two of the five testis datasets might be due to differences in extraction and sample processing methods across the studies. Taken together, these results support the fact that QRICH2 is a testis-specific protein.

QRICH2 immunostaining was observed in all germ cell stages in both IF and IHC on testis sections (Figure 5, and Supplementary Figures S15 and S16, see online Supplementary material). To investigate the temporal dynamics of QRICH2 localization during spermatogenesis, using IF, we performed counter-labeling of testis sections with PSA to visualize sperm acrosomes, thereby identifying germ cell stages during spermiogenesis, or with anti-vimentin to highlight Sertoli cells. For each cell type, equatorial views from confocal z-stacks are provided to accurately depict the precise localization of the labeling (Figure 5B). In spermatogonia, homogeneous immunostaining was detected in the nucleus. In primary spermatocytes, faint immunoreactivity was present inside the nucleus, accompanied by intense QRICH2 immunostaining around the nuclear perimeter. In round spermatids, QRICH2 immunoreactivity appeared as intense puncta evenly scattered within the nucleus, occasionally extending to perinuclear regions, resembling the pattern observed in primary spermatocytes. Notably, no cytoplasmic immunostaining was detected in spermatogonia, primary spermatocytes, or round spermatids. In early elongated spermatids, very faint immunostaining was observed in both the nucleus and cytoplasm. In contrast, in late elongated spermatids, QRICH2 localization was restricted to the flagellum. Additionally, homogeneous immunostaining was observed around the nuclei of Sertoli cells. Control experiments, in which the primary antibody was omitted, showed no labeling in the testis sections, confirming the specificity of the staining (Supplementary Figures S15 and S16).

In ejaculated sperm, QRICH2 was detected in the apical part of the head, the neck, and the flagellum (Figure 6A). Almost no immunolabelling was observed when the anti-QRICH2 antibodies were replaced with rabbit IgG (Figure 6B). In the head, the immunolabelling appears to be localized between the nucleus and the acrosome (Figure 6C), beneath nearly the entire acrosomal surface in most sperm but restricted to the equatorial segment in some (Figure 6A).

Discussion

QRICH2 has been genetically confirmed to be essential for male fertility in mice, bulls, and humans, with gene KO and loss-of-function mutations leading to defective sperm and complete infertility without evident accompanying symptoms (Kherraf *et al.*, 2019; Shen *et al.*, 2019; Hiltpold *et al.*, 2022). It therefore represents a promising, yet underexplored, target for the development of reversible non-hormonal male contraception. In the present study, we aimed to better characterize human QRICH2 to assess its suitability as a target protein for male contraceptive development.

For the first time, we investigated the primary structure of human QRICH2. Indeed, although several isoforms are described in databases, the isoform comprising 1663 aa (Q9H0J4) is recognized as the canonical isoform in UniProtKB. Moreover, it is usually assumed that it is the one expressed in sperm (Kherraf *et al.*, 2019; Shen *et al.*, 2019; Zhang *et al.*, 2024a). Our MS results clearly indicate that a longer isoform, A0A1B0GW36 (1829 aa) or A0A7P0T7G7 (1887 aa), is present in human sperm. The detection of a single, well-defined, band in western blot analysis supports the presence of only one of these isoforms. Interestingly, the apparent MW of native QRICH2 was higher than that of the three recombinant isoforms fused to a C-terminal 3xFlag tag and expressed in HEK293T cells, even the longest one. In addition, each recombinant isoform also displayed an apparent MW greater than its calculated one. These results suggest that both native and recombinant proteins undergo PTMs that could differ between sperm and HEK293T cells. Since QRICH2 is cytosolic (no signal peptide nor transmembrane domains identified in the primary sequence), these PTMs are presumably not glycosylations, which typically occur in the endoplasmic reticulum. Phosphorylation, although generally adding only a slight additional weight (approximately ±1 kDa per phosphate group), can, when occurring at multiple sites, lead to minor changes in MW (Collins *et al.*, 2007). It can also affect SDS binding, resulting in slower protein migration and a higher apparent MW (Lee *et al.*, 2013; Rozanova *et al.*, 2021). Alternatively, differences in the sensitivity of 3D-folded QRICH2 to denaturation between sperm and HEK293T cells could also explain the observed differences in apparent MW.

We showed that QRICH2 is conserved across mammals, and that QRICH2-like proteins are present in vertebrates and other eukaryotes, suggesting functional importance. However, to the best of our knowledge, QRICH2 has not yet been investigated in organisms other than humans, mice, bulls, and goats (Kherraf *et al.*, 2019; Shen *et al.*, 2019; Wang *et al.*, 2020; Hiltpold *et al.*, 2022), limiting our ability to infer its function in other species. Interestingly, the most conserved region includes the C-terminal part of the SMC region and the DUF4795 domain. The function of these domains in sperm is not known yet. According to CDD, DUF4795 has been described in proteins found in bacteria and eukaryotes, but these proteins are functionally uncharacterized. Structural maintenance of chromosomes (SMC) proteins constitute a family of ATPases in Bacteria, Archaea, and Eukaryota. They are part of two protein complexes, cohesin and condensin, that support chromosome condensation, cohesion, and repair (Harvey *et al.*, 2002; Hirano, 2005). These proteins usually comprise between 1,000 and 1,400 aa and contain five domains: C- and N-terminal domains of ∼150 aa involved in DNA binding, and a central region composed of two coiled-coil domains (∼350 aa)

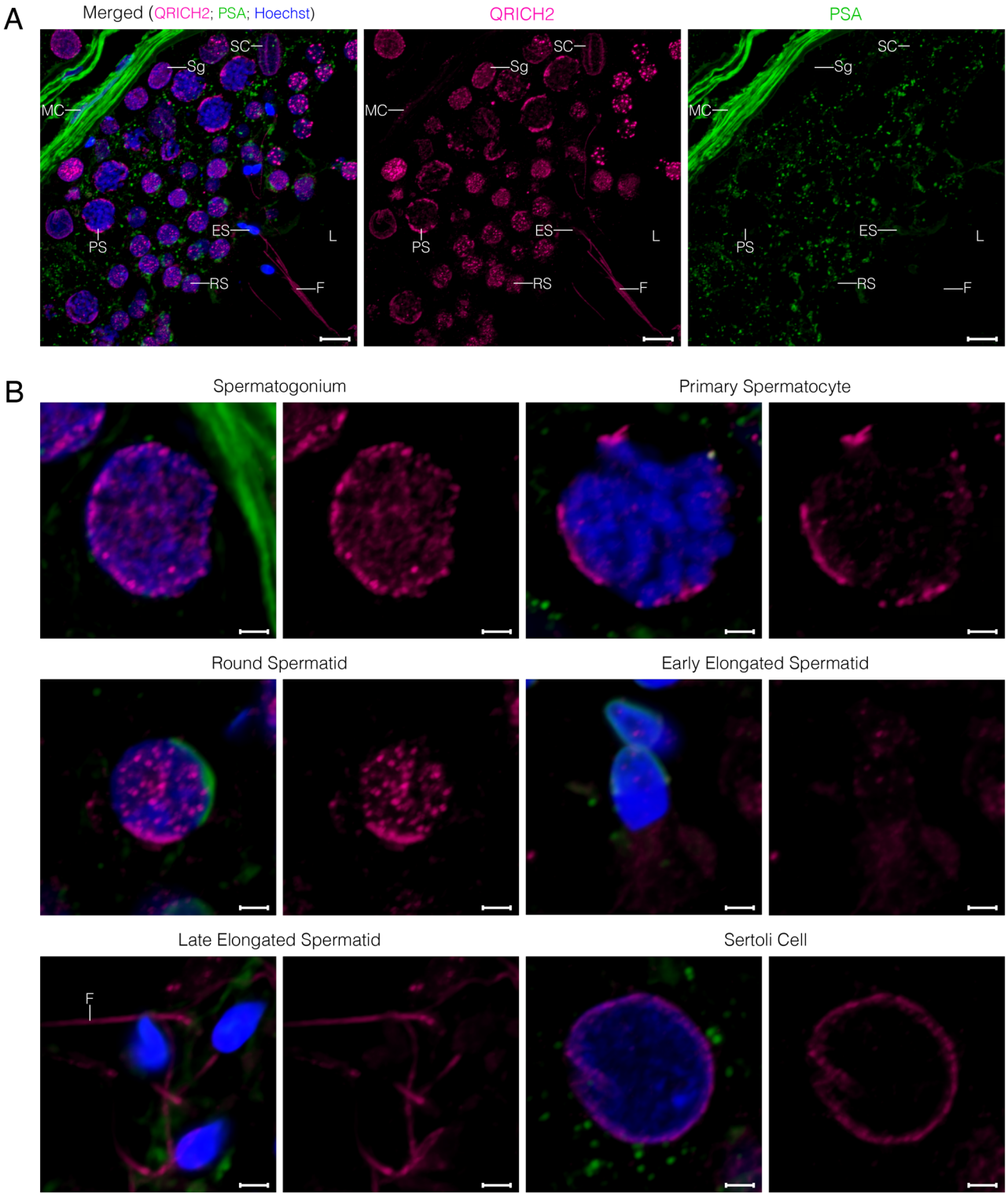

Figure 5 Localization of QRICH2 on human testis sections. (A) Maximum-intensity projections (MaxIP) obtained from z-stack images using Nikon NIS Elements software. (B) Equatorial views of each cell type extracted from the z-stack images. Magenta: QRICH2. Blue: Hoechst staining of the nucleus. Green: PSA-FITC staining (used to visualize sperm acrosomes). Scale bar: 10 µm in (A), 2 µm in (B). ES = Elongated spermatid; F = flagellum; L = lumen of the seminiferous tubule; MC = myoid cell; PS = primary spermatocyte; RS = round spermatid; SC = Sertoli cell; Sg = spermatogonium. Results from another replicate and control are available in Supplementary Figure S15, see online supplementary material.

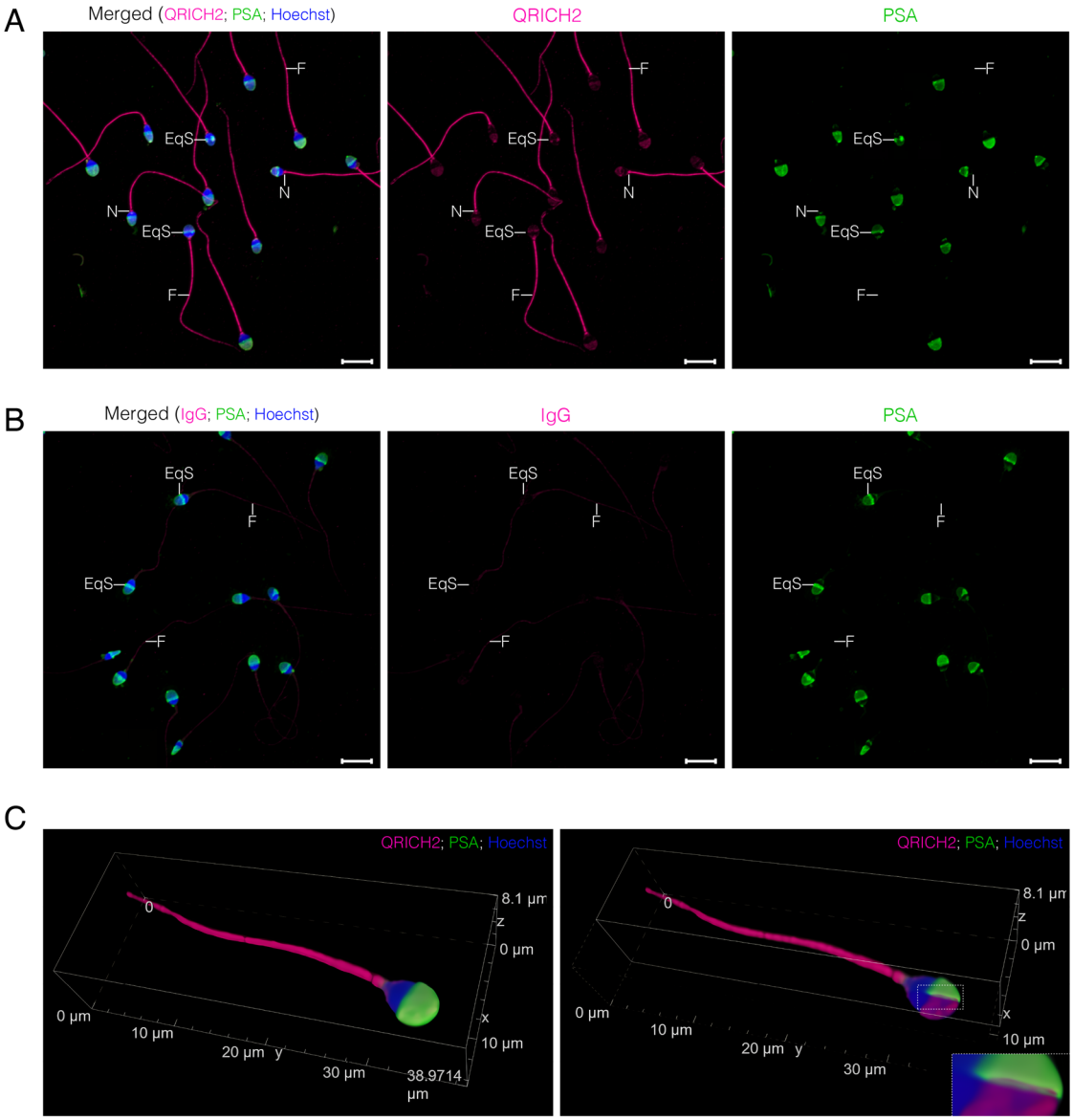

Figure 6 Localization of QRICH2 on ejaculated sperm. (A) QRICH2 and (B) control IgG immunolabeling of ejaculated sperm. Images are maximum-intensity projections (MaxIP) obtained from z-stack images using Nikon NIS Elements software. Scale bar: 10 µm. EqS = Equatorial segment; F = flagellum; N = neck. (C) 3D reconstruction of ejaculated sperm showing the localization of QRICH2. 3D rendered confocal z-stack was obtained using Nikon NIS Elements software. Full rendering is shown on the left. For better clarity, partial rendering with orthogonal planar sectioning applied along the *z*-axis, leaving QRICH2 and nucleus channel unaffected, is shown on the right. This includes an inset that provides a detailed examination of the successive layers in sperm head. The scale is shown on the edge of the box enclosing the sperm. Magenta: QRICH2. Blue: Hoechst staining of the nucleus. Green: PSA-FITC staining (used to visualize sperm acrosomes).

separated by a hinge domain (=200 aa) (Hirano, 2002; Jessberger, 2002). In QRICH2, the sequence with homology to these proteins only comprises 368 aa that appear to be localized in the second coiled-coil domain of SMC proteins from bacteria. Interestingly, ODF2, a main component of flagellum outer dense fibers, and a known interactor of QRICH2 (Shen *et al.*, 2019), also contains an SMC domain. SMC proteins are known to dimerize. It is possible that, in QRICH2, the SMC domain is involved not in chromosome maintenance but in its interaction with other proteins, such as ODF2. In addition to the well-conserved SMC and DU4795 domains, QRICH2 contains a region rich in glycine, glutamine, and proline with similarity to the superfamily of high MW glutenin subunit (Glutenin hmw). High MW glutenin subunits are gluten proteins widely recognized for their elastic properties. They consist of a central elastomeric domain, rich in repeat units of glycine and hydrophobic residues, flanked by non-elastomeric domains that mediate cross-linking between subunits (Tatham & Shewry, 2000). This region could therefore provide elastic properties to QRICH2. Our alignment analyses showed that the glutenin-like domain is highly conserved among mammals and remains less conserved in vertebrates and eukaryotes. Although conservation decreases outside mammals, gap coverage does not drop substantially, indicating that this domain likely retains structural importance across lineages.

To investigate the presence of QRICH2 paralogs in humans, we performed a BLASTp search in the *H. sapiens* database. This search

returned only three hits, but these proteins aligned with only a small region of QRICH2, with low sequence identity. For two of them, SATL1 and piccolo/aczonin, the aligned region corresponded to the Glutenin hmw. According to the HPA, the SATL1 gene is mainly expressed in the testis, albeit at a low expression level, while piccolo/aczonin is ubiquitously expressed. The third protein, uncharacterized protein c16orf96, only aligns with the DUF4795 domain. According to the HPA, the mRNA coding for this protein is enriched in the testis. To the best of our knowledge, the roles of SATL1 and c16orf96 in the testis have not yet been investigated. As for piccolo/aczonin, it appears to regulate calcium-mediated acrosome reaction in mouse sperm (Weber *et al.*, 2014). The restricted alignment regions and low identity suggest that these proteins are not true paralogs of QRICH2 but instead share only some of its domains.

Using immunohistological methods and analysis of 49 proteome datasets, we investigated the tissue specificity of QRICH2 by examining its expression (at the protein level) across 12 human organs: testis, epididymis, brain, heart, colon, pancreas, lung, kidney, thyroid, liver, skin, and prostate. Results showed that QRICH2 is restricted to the testes, consistent with the IHC results available in the HPA database. Noteworthy, while QRICH2 mRNA appears exclusively testicular in mice (Shen *et al.* (2019), MRG, NCBI Gene), in humans, some databases (MRG, HPA, BGee) report low QRICH2 mRNA levels in other tissues. This discrepancy between mRNA and protein localization is not unexpected, as mRNA levels often fail to predict protein abundance due to post-transcriptional regulation and tissue-specific protein stability (Bauernfeind & Babbitt, 2017; Jiang *et al.*, 2020). Altogether, the collected data strongly suggest QRICH2 protein is exclusively expressed in the testes in both humans and mice.

In the testis, QRICH2 is expressed from the spermatogonial stage and is localized at the level of the nucleus in spermatogonia, spermatocytes, and round spermatids, in both the nucleus and cytoplasm in early elongating spermatids, and in the flagellum of elongated spermatids. These results are in line with those described in mice (Shen *et al.*, 2019) and suggest that QRICH2 may play distinct roles at different stages of spermatogenesis. The nuclear localization of QRICH2 aligns with its proposed role as a transcription factor activating the transcription of ODF2 and CABYR by binding to their promotor (Shen *et al.*, 2019) and could be attributed to the presence of two predicted nuclear localization signals (NLS) within its sequence (unpublished observation). The presence of QRICH2 in the flagellum was not surprising either given its known involvement in flagellum biogenesis and the regulation of tubulin glutamylation (Shen *et al.*, 2019; Zhang *et al.*, 2024a). A light QRICH2 immunoreactivity was also observed around the nucleus of Sertoli cells, suggesting that QRICH2 may be expressed in these cells.

In ejaculated sperm, QRICH2 remains mainly localized in the neck and flagellum. The requirement of strong denaturing buffers to extract QRICH2 from sperm suggests that it is highly stabilized within the flagellum, possibly through interactions with cytoskeletal proteins. Indeed, interactions between QRICH2 and proteins from the flagellum axoneme (TUBA, CFAP70) and accessory structures (AKAP3, AKAP4, ODF2, and TSSK4) have been reported in the literature (Shen *et al.*, 2019; Zhang *et al.*, 2021; 2024a; Jin *et al.*, 2023). QRICH2 immunoreactivity was also detected in the sperm head, between the nucleus and the acrosome, beneath nearly the entire acrosomal surface in most sperm, but restricted to the equatorial segment in some. This labelling corresponds to the subacrosomal layer (SAL) of the perinuclear theca, a dense cytoskeletal structure surrounding the sperm nucleus and resistant to non-ionic detergents (Oko & Sutovsky, 2009). These findings are consistent with those of Zhang *et al.* (2022), who identified QRICH2 by MS in the perinuclear theca of boar sperm. SAL proteins are known to originally attach to proacrosomic and acrosomic vesicles during spermiogenesis and, once acrosome biogenesis is over, remain trapped in the SAL (Zhang *et al.*, 2022). The faint QRICH2 immunolabelling detected in the cytoplasm of early elongated spermatids is consistent with its localisation on these vesicles. QRICH2 could therefore play a role in acrosomic vesicle formation, transport, and/or nuclear docking. In mature sperm, it could contribute to binding the acrosome to the nucleus. However, it is difficult to explain why we did not detect QRICH2 in the head of late elongated spermatids. Noteworthy, PSA-FITC labeling of the acrosomes was also absent in most of these cells, indicating a potential bias during the experimentation.

In conclusion, QRICH2 appears as a versatile protein, localized to different cellular compartments throughout spermatogenesis, and functions as a cytoskeletal component in mature sperm, both in the head and the flagellum. Its testis-specific expression, lack of paralogs in other tissues, and the observation that its loss in mice (Shen *et al.*, 2019) and humans (Kherraf *et al.*, 2019; Shen *et al.*, 2019) is not associated with other clinical abnormalities suggest that QRICH2 represents a promising and potentially safe target for male contraception. Its high degree of conservation, along with the availability of validated KO mouse models, supports the feasibility of advancing this research in animal models. Future studies should be dedicated to finding ways to selectively inhibit QRICH2 function, with subsequent investigations needed to evaluate the reversibility and safety of such interventions. Although QRICH2 is not a conventional target for inhibitory molecules (i.e., it is not an enzyme or ion channel), various strategies could be employed to inhibit its function. First, one could focus on inhibiting the ATPase activity of its SMC domain, although further studies are needed to determine whether QRICH2 retains this enzymatic activity. Second, provided that a molecule with high affinity for QRICH2 is discovered, the proteolysis targeting chimera technology could be used to eliminate QRICH2 via the ubiquitin-proteasome pathway (Kent *et al.*, 2020). However, as QRICH2 is already expressed in spermatogonia, complete disruption could result in irreversible infertility. Finally, targeting interactions between QRICH2 and its protein partners may provide an effective means of inhibition, as demonstrated for other protein–protein interactions (PPIs) critical to male fertility (e.g., Chang *et al.*, 2021; Stepanenko *et al.*, 2022). While PPIs are traditionally considered challenging targets for drug discovery, they offer key opportunities to expand the druggable proteome. Recent progress in computational biology have led researchers to reconsider PPIs as viable targets in drug discovery (Rehman *et al.*, 2023). In our laboratory, we are currently investigating QRICH2's interactome. This strategy would allow prioritization of interactions occurring during the post-meiotic developmental stage (spermiogenesis or in mature spermatozoa), thereby enabling more controlled contraceptive approaches. If successful, targeting QRICH2 could expand the repertoire of non-hormonal male contraceptives, offering specific, potentially reversible options that complement existing methods such as condoms and vasectomy, and addressing the current gap in male contraceptive choices.

Supplementary material

Supplementary material is available at *Reproduction* online.

Author contributions

E.H. and J.D. conceptualized the research; E.H. acquired funding for the research; A.D., E.H., M.I., J.D., and T.M. performed the experiments and acquired data for the research; E.H., B.L., and J.D. developed the methodology of the research; E.H. was in charge of the research administration; A.F., B.L., J.-F.S., D.N., V.A., and R.W. provided resources (materials, reagent, patient sample, instrumentation and analysis tools) for the research; E.H. supervised the research; E.H., J.D., and T.M. prepared the data for visualization and wrote the original draft. All authors read, reviewed, and approved the final version of the manuscript.

Conflicts of interest

The authors have declared that there is no conflict of interest that could be perceived as prejudicing the impartiality of the research reported.

Funding

This work was funded by UMONS Research Institute for Biosciences, by the Fund for Scientific Research of Belgium (F.R.S.- FNRS) under Research Credit J.0109.25, by the Walloon Region for the acquisition of the Nikon TI2-E-A1RHD25 confocal microscope, and by the European Regional Development Fund and the Walloon Region as part of support for the Bioprofiling platform, Belgium. T.M. is a FRIA grantee of the F.R.S.–FNRS. J.D. is a Research Associate of the F.R.S.–FNRS.

Acknowledgments

We thank P. Quenon from the Laboratory of Cell Biology in UMONS for technical assistance and all the technicians of the fertility clinic of the HELORA Hospital for their help in the recruitment of patients and voluntary donors.

Data availability

The data underlying this article are available in the article and its online supplementary material.

References

Altschul, S. F., Gish, W., Miller, W., Myers, E. W., & Lipman, D. J. (1990). Basic local alignment search tool. *Journal of Molecular Biology*, *215*, 403–410. https://doi.org/10.1016/S0022-2836(05)80360-2

Bauernfeind, A. L., & Babbitt, C. C. (2017). The predictive nature of transcript expression levels on protein expression in adult human brain. *BMC Genomics*, *18*, 322. https://doi.org/10.1186/s12864-017-3674-x

Capra, J. A., & Singh, M. (2007). Predicting functionally important residues from sequence conservation. *Bioinformatics (Oxford, England)*, *23*, 1875–1882. https://doi.org/10.1093/bioinformatics/btm270

Chang, Z., Qin, W., Zheng, H., Schegg, K., Han, L., Liu, X., Wang, Y., Wang, Z., McSwiggin, H., Peng, H., Yuan, S., Wu, J., Wang, Y., Zhu, S., Jiang, Y., Nie, H., Tang, Y., Zhou, Y., Hitchcock, M. J. M., … Yan, W. (2021). Triptonide is a reversible non-hormonal male contraceptive agent in mice and non-human primates. *Nature Communications*, *12*, 1253. https://doi.org/10.1038/s41467-021-21517-5

Collins, M. O., Yu, L., & Choudhary, J. S. (2007). Analysis of protein phosphorylation on a proteome-scale. *Proteomics*, *7*, 2751–2768. https://doi.org/10.1002/pmic.200700145

Deutsch, E. W., Bandeira, N., Perez-Riverol, Y., *et al.* (2023). The ProteomeXchange consortium at 10 years: 2023 update. *Nucleic Acids Research*, *51*, D1539–D1548. https://doi.org/10.1093/nar/gkac1040

Harvey, S. H., Krien, M. J., & O'connell, M. J. (2002). Structural maintenance of chromosomes (SMC) proteins, a family of conserved ATPases. *Genome Biology*, *3*, reviews3003.1. https://doi.org/10.1186/gb-2002-3-2-reviews3003

Hiltpold, M., Janett, F., Mapel, X. M., *et al.* (2022). A 1-bp deletion in bovine QRICH2 causes low sperm count and immotile sperm with multiple morphological abnormalities. *Genetics Selection Evolution*, *54*, 18. https://doi.org/10.1186/s12711-022-00710-0

Hirano, T. (2002). The ABCs of SMC proteins: Two-armed ATPases for chromosome condensation, cohesion, and repair. *Genes & Development*, *16*, 399–414. https://doi.org/10.1101/gad.955102

Hirano, T. (2005). SMC proteins and chromosome mechanics: From bacteria to humans. *Philosophical Transactions of the Royal Society of London. Series B, Biological Sciences*, *360*, 507–514. https://doi.org/10.1098/rstb.2004.1606

Jessberger, R. (2002). The many functions of SMC proteins in chromosome dynamics. *Nature Reviews. Molecular Cell Biology*, *3*, 767–778. https://doi.org/10.1038/nrm930

Jiang, L., Wang, M., Lin, S., *et al.* (2020). A quantitative proteome map of the human body. *Cell*, *183*, 269–283.e19. https://doi.org/10.1016/j.cell.2020.08.036

Jin, H.-J., Wang, J.-L., Geng, X.-Y., Wang, C.-Y., Wang, B.-B., & Chen, S.-R. (2023). CFAP70 is a solid and valuable target for the genetic diagnosis of oligo-astheno-teratozoospermia in infertile men. *EBioMedicine*, *93*, 104675. https://doi.org/10.1016/j.ebiom.2023.104675

Katoh, K., Rozewicki, J., & Yamada, K. D. (2017). MAFFT online service: Multiple sequence alignment, interactive sequence choice and visualization. *Briefings in Bioinformatics*, *20*, 1160–1166. https://doi.org/10.1093/bib/bbx108

Kent, K., Johnston, M., Strump, N., *et al.* (2020). Toward development of the male pill: A decade of potential non-hormonal contraceptive targets. *Frontiers in Cell and Developmental Biology*, *8*, 61. https://doi.org/10.3389/fcell.2020.00061

Kherraf, Z.-E., Cazin, C., Coutton, C., Amiri-Yekta, A., Martinez, G., Boguenet, M., Fourati Ben Mustapha, S., Kharouf, M., Gourabi, H., Hosseini, S. H., Daneshipour, A., Touré, A., Thierry-Mieg, N., Zouari, R., Arnoult, C., & Ray, P. F. (2019). Whole exome sequencing of men with multiple morphological abnormalities of the sperm flagella reveals novel homozygous QRICH2 mutations. *Clinical Genetics*, *96*, 394–401. https://doi.org/10.1111/cge.13604

Khilwani, B., Badar, A., Ansari, A. S., & Lohiya, N. K. (2020). RISUG® as a male contraceptive: Journey from bench to bedside. *Basic and Clinical Andrology*, *30*, 2. https://doi.org/10.1186/s12610-020-0099-1

Kim, J., So, B., Heo, Y., So, H., & Jo, J. K. (2024). Advances in male contraception: When will the novel male contraception be available? *The World Journal of Men's Health*, *42*, 487–501. https://doi.org/10.5534/wjmh.230118

Kriventseva, E. V., Kuznetsov, D., Tegenfeldt, F., Manni, M., Dias, R., Simão, F. A., & Zdobnov, E. M. (2019). OrthoDB v10: Sampling the diversity of animal, plant, fungal, protist, bacterial and viral genomes for evolutionary and functional annotations of orthologs. *Nucleic Acids Research*, *47*, D807–D811. https://doi.org/10.1093/nar/gky1053

Lamesch, P., Li, N., Milstein, S., Fan, C., Hao, T., Szabo, G., Hu, Z., Venkatesan, K., Bethel, G., Martin, P., Rogers, J., Lawlor, S., McLaren, S., Dricot, A., Borick, H., Cusick, M. E., Vandenhaute, J., Dunham, I., Hill, D. E., & Vidal, M. (2007). hORFeome v3.1: A resource of human open reading frames representing over 10,000 human genes. *Genomics*, *89*, 307–315. https://doi.org/10.1016/j.ygeno.2006.11.012

Lee, C.-R., Park, Y.-H., Kim, Y.-R., *et al.* (2013). Phosphorylation-dependent mobility shift of proteins on SDS-PAGE is due to decreased binding of SDS. *Bulletin of the Korean Chemical Society*, *34*, 2063–2066. https://doi.org/10.5012/bkcs.2013.34.7.2063

Liu, W., Xie, Y., Ma, J., Luo, X., Nie, P., Zuo, Z., Lahrmann, U., Zhao, Q., Zheng, Y., Zhao, Y., Xue, Y., & Ren, J. (2015). IBS: An illustrator for the presentation and visualization of biological sequences. *Bioinformatics (Oxford, England)*, *31*, 3359–3361. https://doi.org/10.1093/bioinformatics/btv362

Lohiya, N. K., Ansari, A. S., Sadasukhi, T. C., *et al.* (2022). RISUG® offers early contraception: An experience during Phase III clinical trials. *Journal of Reproductive Healthcare and Medicine*, *3*, 11. https://doi.org/10.25259/JRHM_8_2022

Louwagie, E. J., Quinn, G. F. L., Pond, K. L., & Hansen, K. A. (2023). Male contraception: Narrative review of ongoing research. *Basic and Clinical Andrology*, *33*, 30. https://doi.org/10.1186/s12610-023-00204-z

Nicholson, C. M., Abramsson, L., Holm, S. E., & Bjurulf, E. (2000). Bacterial contamination and sperm recovery after semen preparation by density gradient centrifugation using silane-coated silica particles at different g forces. *Human Reproduction (Oxford, England)*, *15*, 662–666. https://doi.org/10.1093/humrep/15.3.662

Nickels, L., & Yan, W. (2024). Nonhormonal male contraceptive development-strategies for progress. *Pharmacological Reviews*, *76*, 37–48. https://doi.org/10.1124/pharmrev.122.000787

Oko, R., & Sutovsky, P. (2009). Biogenesis of sperm perinuclear theca and its role in sperm functional competence and fertilization. *Journal of Reproductive Immunology*, *83*, 2–7. https://doi.org/10.1016/j.jri.2009.05.008

ORFeome Collaboration, C. (2016). The ORFeome Collaboration: A genome-scale human ORF-clone resource. *Nature Methods*, *13*, 191–192. https://doi.org/10.1038/nmeth.3776

Rehman, A. U., Khurshid, B., Ali, Y., Rasheed, S., Wadood, A., Ng, H.-L., Chen, H.-F., Wei, Z., Luo, R., & Zhang, J. (2023). Computational approaches for the design of modulators targeting protein-protein interactions. *Expert Opinion on Drug Discovery*, *18*, 315–333. https://doi.org/10.1080/17460441.2023.2171396

Rozanova, S., Barkovits, K., Nikolov, M., Schmidt, C., Urlaub, H., & Marcus, K. (2021). Quantitative mass spectrometry-based proteomics: An overview. *Methods in Molecular Biology (Clifton, N.J.)*, *2228*, 85–116. https://doi.org/10.1007/978-1-0716-1024-4_8

Shen, Y., Zhang, F., Li, F., Jiang, X., Yang, Y., Li, X., Li, W., Wang, X., Cheng, J., Liu, M., Zhang, X., Yuan, G., Pei, X., Cai, K., Hu, F., Sun, J., Yan, L., Tang, L., Jiang, C.Xu, W. (2019). Loss-of-function mutations in QRICH2 cause male infertility with multiple morphological abnormalities of the sperm flagella. *Nature Communications*, *10*, 433. https://doi.org/10.1038/s41467-018-08182-x

Stepanenko, N., Wolk, O., Bianchi, E., *et al.* (2022). In silico docking analysis for blocking JUNO-IZUMO1 interaction identifies two small molecules that block in vitro fertilization. *Frontiers in Cell and Developmental Biology*, *10*, 824629. https://doi.org/10.3389/fcell.2022.824629

Sun, J., Shi, J., Wang, Y., *et al.* (2019). Open-pFind enhances the identification of missing proteins from human testis tissue. *Journal of Proteome Research*, *18*, 4189–4196. https://doi.org/10.1021/acs.jproteome.9b00376

Tatham, A. S., & Shewry, P. R. (2000). Elastomeric proteins: Biological roles, structures and mechanisms. *Trends in Biochemical Sciences*, *25*, 567–571. https://doi.org/10.1016/S0968-0004(00)01670-4

Thirumalai, A., & Page, S. T. (2020). Male hormonal contraception. *Annual Review of Medicine*, *71*, 17–31. https://doi.org/10.1146/annurev-med-042418-010947

Thirumalai, A., & Amory, J. K. (2021). Emerging approaches to male contraception. *Fertility and Sterility*, *115*, 1369–1376. https://doi.org/10.1016/j.fertnstert.2021.03.047

Wang, C., Festin, M. P., & Swerdloff, R. S. (2016). Male hormonal contraception: Where are we now? *Current Obstetrics and Gynecology Reports*, *5*, 38–47. https://doi.org/10.1007/s13669-016-0140-8

Wang, J., Chitsaz, F., Derbyshire, M. K., Gonzales, N. R., Gwadz, M., Lu, S., Marchler, G. H., Song, J. S., Thanki, N., Yamashita, R. A., Yang, M., Zhang, D., Zheng, C., Lanczycki, C. J., & Marchler-Bauer, A. (2023). The conserved domain database in 2023. *Nucleic Acids Research*, *51*, D384–D388. https://doi.org/10.1093/nar/gkac1096

Wang, Z., Pan, Y., He, L., Song, X., Chen, H., Pan, C., Qu, L., Zhu, H., & Lan, X. (2020). Multiple morphological abnormalities of the sperm flagella (MMAF)-associated genes: The relationships between genetic variation and litter size in goats. *Gene*, *753*, 144778. https://doi.org/10.1016/j.gene.2020.144778

Weber, N., Vieweg, L., Henze, F., Oprisoreanu, A.-M., Solinski, H. J., Breit, A., Fecher-Trost, C., Schalkowsky, P., Wilhelm, B., Wennemuth, G., Schoch, S., Gudermann, T., & Boekhoff, I. (2014). RIM2alpha is a molecular scaffold for Zona pellucida-induced acrosome reaction. *Journal of Molecular Cell Biology*, *6*, 434–437. https://doi.org/10.1093/jmcb/mju037

WHO. (2021). *WHO laboratory manual for the examination and processing of human semen* (6th ed., 276 pages). World Health Organization.

Wingfield, P. T. (2017). N-terminal methionine processing. *Current Protocols in Protein Science*, *88*, 6141–6143.

Zhang, G., Li, D., Tu, C., Meng, L., Tan, Y., Ji, Z., Cheng, J., Lu, G., Lin, G., Zhang, H., Sun, J., Wang, M., Du, J., & Xu, W. (2021). Loss-of-function missense variant of AKAP4 induced male infertility through reduced interaction with QRICH2 during sperm

flagella development. *Human Molecular Genetics*, *31*, 219–231. https://doi.org/10.1093/hmg/ddab234

Zhang, G., Guo, J., Yang, H., Li, Q., Ye, F., Song, Y., Xiong, D., Zeng, J., Zhi, W., Yuan, S., Lv, Y., Li, T., Wang, Y., Liao, L., Deng, D., Liu, W., & Xu, W. (2024a). Metabolic profiling identifies Qrich2 as a novel glutamine sensor that regulates microtubule glutamylation and mitochondrial function in mouse sperm. *Cellular and Molecular Life Sciences: CMLS*, *81*, 170. https://doi.org/10.1007/s00018-024-05177-4

Zhang, G., Xiong, D., Ye, F., *et al.* (2024b). A Key regulatory protein QRICH2 governing sperm function with profound antioxidant properties, enhancing sperm viability. *Reproductive Biology*, *24*, 100881. https://doi.org/10.1016/j.repbio.2024.100881

Zhang, M., Chiozzi, R. Z., Skerrett-Byrne, D. A., Veenendaal, T., Klumperman, J., Heck, A. J. R., Nixon, B., Helms, J. B., Gadella, B. M., & Bromfield, E. G. (2022). High resolution proteomic analysis of subcellular fractionated boar spermatozoa provides comprehensive insights into perinuclear theca-residing proteins. *Frontiers in Cell and Developmental Biology*, *10*, 836208. https://doi.org/10.3389/fcell.2022.836208

Zheng, W., Zhang, Y., Sun, C., *et al.* (2021). A multi-omics study of human testis and epididymis. *Molecules*, *26*, 3345. https://doi.org/10.3390/molecules26113345